Radiative decay of the $\psi(2S)$ into two pseudoscalar mesons

J. Z. Bai,[1] Y. Ban,[11] J. G. Bian,[1] I. Blum,[19] A. D. Chen,[1] G. P. Chen,[1] H. F. Chen,[18] H. S. Chen,[1] J. Chen,[5] J. C. Chen,[1] X. D. Chen,[1] Y. Chen,[1] Y. B. Chen,[1] B. S. Cheng,[1] J. B. Choi,[4] X. Z. Cui,[1] H. L. Ding,[1] L. Y. Dong,[1] Z. Z. Du,[1] W. Dunwoodie,[15] C. S. Gao,[1] M. L. Gao,[1] S. Q. Gao,[1] P. Gratton,[19] J. H. Gu,[1] S. D. Gu,[1] W. X. Gu,[1] Y. N. Guo,[1] Z. J. Guo,[1] S. W. Han,[1] Y. Han,[1] F. A. Harris,[16] J. He,[1] J. T. He,[1] K. L. He,[1] M. He,[12] Y. K. Heng,[1] D. G. Hitlin,[2] G. Y. Hu,[1] H. M. Hu,[1] J. L. Hu,[1] Q. H. Hu,[1] T. Hu,[1] G. S. Huang,[3] X. P. Huang,[1] Y. Z. Huang,[1] J. M. Izen,[19] C. H. Jiang,[1] Y. Jin,[1] B. D. Jones,[19] X. Ju,[1] J. S. Kang,[9] Z. J. Ke,[1] M. H. Kelsey,[2] B. K. Kim,[19] H. J. Kim,[14] S. K. Kim,[14] T. Y. Kim,[14] D. Kong,[16] Y. F. Lai,[1] P. F. Lang,[1] A. Lankford,[17] C. G. Li,[1] D. Li,[1] H. B. Li,[1] J. Li,[1] J. C. Li,[1] P. Q. Li,[1] W. Li,[1] W. G. Li,[1] X. H. Li,[1] X. N. Li,[1] X. Q. Li,[10] Z. C. Li,[1] B. Liu,[1] F. Liu,[8] Feng. Liu,[1] H. M. Liu,[1] J. Liu,[1] J. P. Liu,[20] R. G. Liu,[1] Y. Liu,[1] Z. X. Liu,[1] X. C. Lou,[19] B. Lowery,[19] G. R. Lu,[7] F. Lu,[1] J. G. Lu,[1] X. L. Luo,[1] E. C. Ma,[1] J. M. Ma,[1] R. Malchow,[5] H. S. Mao,[1] Z. P. Mao,[1] X. C. Meng,[1] X. H. Mo,[1] J. Nie,[1] S. L. Olsen,[16] J. Oyang,[2] D. Paluselli,[16] L. J. Pan,[16] J. Panetta,[2] H. B. Park,[9] F. Porter,[2] N. D. Qi,[1] X. R. Qi,[1] C. D. Qian,[13] J. F. Qiu,[1] Y. H. Qu,[1] Y. K. Que,[1] G. Rong,[1] M. Schernau,[17] Y. Y. Shao,[1] B. W. Shen,[1] D. L. Shen,[1] H. Shen,[1] H. Y. Shen,[1] X. Y. Shen,[1] F. Shi,[1] H. Z. Shi,[1] X. F. Song,[1] J. Standifird,[19] J. Y. Suh,[9] H. S. Sun,[1] L. F. Sun,[1] Y. Z. Sun,[1] S. Q. Tang,[1] W. Toki,[5] G. L. Tong,[1] G. S. Varner,[16] F. Wang,[1] L. Wang,[1] L. S. Wang,[1] L. Z. Wang,[1] P. Wang,[1] P. L. Wang,[1] S. M. Wang,[1] Y. Y. Wang,[1] Z. Y. Wang,[1] M. Weaver,[2] C. L. Wei,[1] N. Wu,[1] Y. G. Wu,[1] D. M. Xi,[1] X. M. Xia,[1] Y. Xie,[1] Y. H. Xie,[1] G. F. Xu,[1] S. T. Xue,[1] J. Yan,[1] W. G. Yan,[1] C. M. Yang,[1] C. Y. Yang,[1] H. X. Yang,[1] W. Yang,[5] X. F. Yang,[1] M. H. Ye,[1] S. W. Ye,[18] Y. X. Ye,[18] C. S. Yu,[1] C. X. Yu,[1] G. W. Yu,[1] Y. H. Yu,[6] Z. Q. Yu,[1] C. Z. Yuan,[1] Y. Yuan,[1] B. Y. Zhang,[1] C. Zhang,[1] C. C. Zhang,[1] D. H. Zhang,[1] Dehong Zhang,[1] H. L. Zhang,[1] J. Zhang,[1] J. W. Zhang,[1] L. Zhang,[1] Lei. Zhang,[1] L. S. Zhang,[1] P. Zhang,[1] Q. J. Zhang,[1] S. Q. Zhang,[1] X. Y. Zhang,[12] Y. Y. Zhang,[1] D. X. Zhao,[1] H. W. Zhao,[1] Jiawei Zhao,[18] J. W. Zhao,[1] M. Zhao,[1] W. R. Zhao,[1] Z. G. Zhao,[1] J. P. Zheng,[1] L. S. Zheng,[1] Z. P. Zheng,[1] B. Q. Zhou,[1] L. Zhou,[1] K. J. Zhu,[1] Q. M. Zhu,[1] Y. C. Zhu,[1] Y. S. Zhu,[1] Z. A. Zhu,[1] and B. A. Zhuang[1]

(BES Collaboration)

[1]*Institute of High Energy Physics, Beijing 100039, People's Republic of China*
[2]*California Institute of Technology, Pasadena, California 91125*
[3]*China Center of Advanced Science and Technology, Beijing 100087, People's Republic of China*
[4]*Chonbuk National University, Republic of Korea*
[5]*Colorado State University, Fort Collins, Colorado 80523*
[6]*Hangzhou University, Hangzhou 310028, People's Republic of China*
[7]*Henan Normal University, Xinxiang 453002, People's Republic of China*
[8]*Huazhong Normal University, Wuhan 430079, People's Republic of China*
[9]*Korea University, Republic of Korea*
[10]*Nankai University, Tianjin 300071, People's Republic of China*
[11]*Peking University, Beijing 100871, People's Republic of China*
[12]*Shandong University, Jinan 250100, People's Republic of China*
[13]*Shanghai Jiaotong University, Shanghai 200030, People's Republic of China*
[14]*Seoul National University, Republic of Korea*
[15]*Stanford Linear Accelerator Center, Stanford, California 94309*
[16]*University of Hawaii, Honolulu, Hawaii 96822*
[17]*University of California at Irvine, Irvine, California 92717*
[18]*University of Science and Technology of China, Hefei 230026, People's Republic of China*
[19]*University of Texas at Dallas, Richardson, Texas 75083-0688*
[20]*Wuhan University, Wuhan 430072, People's Republic of China*

Radiative decays of the radially excited charmonium resonance, $\psi(2S)$, into $\pi\pi$, $K\bar{K}$ and $\eta\eta$ final states have been measured in a sample of 4.02×10^6 $\psi(2S)$ events collected by the BES Collaboration. The branching ratios $B(\psi(2S)\rightarrow\gamma f_2(1270))=(2.12\pm0.19\pm0.32)\times10^{-4}$ and $B(\psi(2S)\rightarrow\gamma f_0(1710))\times B(f_0(1710)\rightarrow K^+K^-)=(3.02\pm0.45\pm0.66)\times10^{-5}$ are obtained. When compared to the corresponding radiative J/ψ decays, the observed $\psi(2S)$ radiative decay rates into $\gamma f_2(1270)$ and $\gamma f_0(1710)$ are consistent with the prediction of the "12%" rule.

I. MOTIVATION

In perturbative QCD, the dominant process of J/ψ and $\psi(2S)$ hadronic decay is $c\bar{c}$ annihilation into three gluons. Since the decay width is proportional to the amplitude of the $c\bar{c}$ wave function at the origin, $|\Psi(0)|^2$, the branching fractions of J/ψ and $\psi(2S)$ decays into light quark states are related as [1].

$$\frac{B(\psi(2S)\to h)}{B(J/\psi\to h)}=\frac{B(\psi(2S)\to ggg)}{B(J/\psi\to ggg)}$$

$$\simeq\frac{B(\psi(2S)\to e^+e^-)}{B(J/\psi\to e^+e^-)}$$

$$=(12.3\pm0.7)\%. \qquad (1)$$

This relation is called *the 12% rule*. The prediction was originally made for the total decay width into three gluons. Since the partial widths of individual channels involving the initial annihilation of $c\bar{c}$ quarks are also functions of the $|\Psi(0)|^2$, we expect this rule to be generally valid.

Results from the Mark II experiment [2] show that while many of the $\psi(2S)$ hadronic decay channels obey this rule, it is severely violated in vector plus pseudoscalar (VP) final states such as $\rho\pi$ and $K^*\bar{K}$—the so-called $\rho\pi$ puzzle. These decays are strongly suppressed and yield ratios $<0.65\%$ and $<1.1\%$ respectively. In the BES experiment [3], we reported heavy suppression in the vector plus tensor (VT) final states such as $K^*\bar{K}_2^*$, ρa_2, ωf_2 and $\phi f_2'$.

In perturbative QCD, the radiative J/ψ and $\psi(2S)$ decays should be similar to hadronic decays except, instead of decaying into three gluons, the radiative mode decays via two gluons and one photon. Thus one power of the coefficient α_S is replaced by α_{QED} in the cross section formula. It is expected that the "12%" rule should also work for radiative decay modes [4]. Hence the ratio of $B(\psi(2S)\to\gamma X)$ to $B(J/\psi\to\gamma X)$ for different final states X should be roughly 12%. This paper explores the $\psi(2S)$ radiative decays into pairs of pseudoscalars, $\pi\pi$, $K\bar{K}$ and $\eta\eta$, and reports the first branching fraction measurements of $\psi(2S)\to\gamma f_2(1270)$ and $\gamma f_0(1710)$. The branching fractions of χ_{c0} and χ_{c2} decays into $\pi\pi$ and $\eta\eta$ are also reported.

The $f_0(1710)$ has been observed with a large branching ratio in radiative decays of J/ψ into $K\bar{K}$, but not in the reaction $K^-p\to KK\Lambda$ by the LASS experiment [5]. The latter result excludes $f_0(1710)$ as a conventional $s\bar{s}$ state and makes it a leading glueball candidate. Thus whether $f_0(1710)$ can be seen in the radiative $\psi(2S)$ decays is quite interesting.

II. BES DETECTOR

This study uses a subset of the 4.02 million $e^+e^-\to\psi(2S)$ events [6] logged by the BES detector operating at the Beijing Electron Positron Collider(BEPC) storage ring at $\sqrt{s}\sim3.686$ GeV. A detailed description of the BES detector can be found elsewhere [7]. It features a 40-layer main drift chamber (MDC) in a 0.4 T solenoidal magnetic field providing a momentum resolution of $\sigma_p/p=1.7\%\sqrt{1+p^2}$(GeV/c) and a dE/dx resolution of 9% for hadron tracks. Outside the MDC cylinder is an array of 48 scintillation counters of the time-of-flight (TOF) system with a resolution of 450 ps for hadrons. A 24-layer lead-gas barrel electromagnetic shower calorimeter (BSC), outside of the TOF system, provides an energy resolution of $\sigma_E/E=0.22/\sqrt{E(\text{GeV})}$, and spatial resolutions of $\sigma_\phi=4.5$ mrad and $\sigma_\theta=12$ mrad (θ and ϕ are the polar angle and azimuthal angle of the cylinder shape detector). The BSC is surrounded by a magnetic coil and steel plates (for magnetic flux return). There is a 3-layer gas proportional tube detector (the μ counter) interleaved with the steel plates to identify μ tracks.

The photons used in this analysis are detected as showers in the BSC. Showers within $8°$ of each other are regarded as split showers of a single photon candidate and their energies are combined. For charged tracks, only those that fall in the fiducial region $|\cos\theta|<0.8$ are used. Charged tracks identified as electrons or positrons by the BSC or identified as μ^+ or μ^- by the μ counter are rejected. TOF information, dE/dx information and kinematic fitting are used to identify charged particles. Kinematic fits are applied to improve momentum measurements and mass resolutions, as well as to resolve combinatorial ambiguities if more than one combination is possible in the same event.

III. $\psi(2S)$ NORMALIZATION

To determine branching fractions, the total number of $\psi(2S)$ events is required. BES determined this number by using the observed number of decays of $\psi(2S)\to\pi^+\pi^-J/\psi$, $J/\psi\to$ anything, and the branching fraction for this decay, $B(\psi(2S)\to\pi^+\pi^-J/\psi)$, which is $(30.5\pm1.6)\%$ [8]. The total number of $\psi(2S)\to\pi^+\pi^-J/\psi$ events observed in the full BES data sample is $(1.227\pm0.003\pm0.017)\times10^6$ [6,9,10]. Because our results depend on $B(\psi(2S)\to\pi^+\pi^-J/\psi)$, this paper also provides ratios of branching fractions to $B(\psi(2S)\to\pi^+\pi^-J/\psi)$. They are obtained from the corrected numbers of events in various channels divided by the corrected number of events of $\psi(2S)\to\pi^+\pi^-J/\psi$, $J/\psi\to$ anything. (See Table III and Table V.)

IV. $\psi(2s)\to\gamma\pi\pi$ ANALYSIS

Here the analysis of decays into both charged and neutral pion pairs, $\psi(2S)\to\gamma\pi^+\pi^-$ and $\psi(2S)\to\gamma\pi^0\pi^0$, is described. In the charged channel, events are selected with two oppositely charged tracks and at least one photon. Kinematic fit, TOF, and dE/dx information are combined, and the probability for the two pion hypothesis is required to be greater than 1% and also to be greater than the joint probability for the two kaon hypothesis. The solid-line histogram of Fig. 1 is the $\pi^+\pi^-$ invariant mass distribution below 2.5 GeV. A clear ρ signal is observed. This ρ signal is not due to $\psi(2S)\to\gamma\rho$ production but is from the initial state radiation process $e^+e^-\to\gamma\rho$. This background and the smooth background from $e^+e^-\to\gamma\mu^+\mu^-$ are also present when we use the same analysis on the $e^+e^-\to\tau\tau$ scan data taken by BES
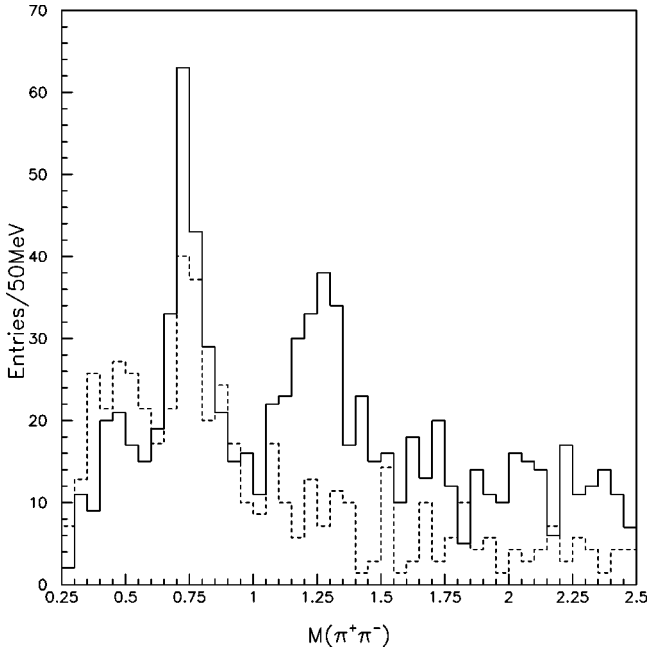
FIG. 1. $M_{\pi^+\pi^-}$ distributions. The solid line histogram is the distribution for the $\psi(2S)$ data; the dashed histogram is that for the normalized τ data.

at $\sqrt{s}=3.55-3.6$ GeV [below $\psi(2S)$ threshold] [11,12], and the mass distribution from the $\tau\tau$ scan can be used to represent these backgrounds in the $\psi(2S)$ sample. The $\pi^+\pi^-$ mass distribution taken from the τ scan data [normalized to the same integrated luminosity as the $\psi(2S)$ data] is also shown in Fig. 1 as the dashed line. In the fitting, the backgrounds are removed by assigning each $\psi(2S)$ event a weight of 1 and each τ event a weight of $-w$ in the likelihood function for the mass fit. Here w is the ratio of the integrated luminosities of these two data sets. Figure 2(a)

shows the result of subtracting the $\tau\tau$ scan histogram normalized to the $\psi(2S)$ from the $\psi(2S)$ histogram.

In the neutral mode, events are required to have at least 5 photon candidates and no charged tracks. A six-constraint fit is made to all possible $\gamma\pi^0\pi^0$ combinations with two π^0 resonances. The combination with the smallest fit χ^2 is selected. A four-constraint fit is also applied on that combination and $|M_{\gamma\gamma}-M_{\pi^0}|<70$ MeV is required. Because radiative background processes that are possible for the charged mode, such as $e^+e^-\to\gamma\rho$ and $\gamma\mu^+\mu^-$, cannot appear in the pure-neutral-track final states, subtraction of the normalized τ data is not needed here. The resulting mass distribution is shown in Fig. 2(b).

In both the $\pi^+\pi^-$ and $\pi^0\pi^0$ invariant mass distributions, clear $f_2(1270)$ signals are observed. Both distributions are fitted with a D-wave Breit-Wigner function with the resonant parameters fixed at the Particle Data Group (PDG) [8] values for the $f_2(1270)$. An S-wave Breit-Wigner with mass and width fixed at the PDG values for the $f_0(1710)$ is included in the mass fitting in the $\gamma\pi^+\pi^-$ channel in order to describe the line shape in that region. A phase space background is included in the $\gamma\pi^0\pi^0$ channel. The fit yields 200.6 ± 18.8 events and 29.9 ± 11.1 events above background, as shown in Fig. 2(a) and Fig. 2(b), respectively.

Branching fractions of $B(\psi(2S)\to\gamma f_2(1270))=(2.08\pm0.19\pm0.33)\times10^{-4}$ from the $\psi(2S)\to\gamma\pi^+\pi^-$ channel and $B(\psi(2S)\to\gamma f_2(1270))=(2.90\pm1.08\pm1.07)\times10^{-4}$ from the $\psi(2S)\to\gamma\pi^0\pi^0$ channel are obtained using the total number of $\psi(2S)$ events and detection efficiencies, which are determined from Monte Carlo simulations, of 43.8% and 9.6%, respectively. The combined result from these two channels is

$$B(\psi(2S)\to\gamma f_2(1270))=(2.12\pm0.19\pm0.32)\times10^{-4}.$$

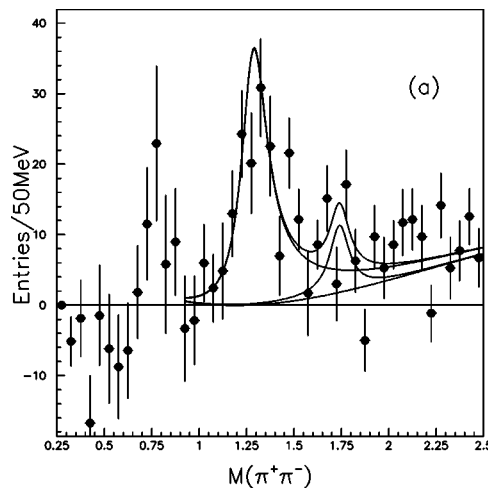Here and below, the first error is statistical and the second is

FIG. 2. (a) $M_{\pi^+\pi^-}$ fit result. The data points are obtained from the difference of the two histograms in Fig. 1. The four curves presented in the figure are the following: a background curve, a Breit-Wigner function to describe the $f_2(1270)$ on top of the background, a Breit-Wigner function to describe the $f_0(1710)$ on top of the background, and the total of the two Breit-Wigner functions and the background. The fitting range is 0.9 GeV to 2.5 GeV, since some ρ background remains below 0.9 GeV. The background at higher mass is due to other processes that are not present in the $e^+e^-\to\tau^+\tau^-$ data, such as $\psi(2S)\to$ neutrals J/ψ, $J/\psi\to\pi^+\pi^-\pi^0$. (b) $M_{\pi^0\pi^0}$ fit result. The curves shown are a Breit-Wigner function to describe the $f_2(1270)$ and a polynomial to describe the background.
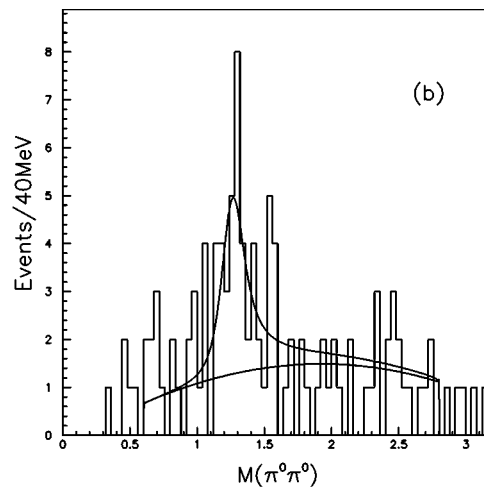
TABLE I. Verification of the 12% rule. The value of $B(J/\psi \to \gamma f_0(1710) \to \gamma K^+ K^-)$ is obtained from $B(J/\psi \to \gamma f_0(1710) \to \gamma K\bar{K}) = (8.5^{+1.2}_{-0.9}) \times 10^{-4}$ divided by a factor of 2 to account for isospin.

Final state	$B(\psi(2S) \to)(\times 10^{-4})$	$B(J/\psi \to)(\times 10^{-4})$	$B(\psi(2S))/B(J/\psi)$
$\gamma f_2(1270)$	$2.12 \pm 0.19 \pm 0.32$	13.8 ± 1.4	$(15.4 \pm 3.1)\%$
$\gamma f_0(1710) \to \gamma K^+ K^-$	$0.302 \pm 0.045 \pm 0.066$	$4.25^{+0.60}_{-0.45}$ [8]	$(7.1^{+2.1}_{-2.0})\%$

systematic. The latter includes uncertainties from varying the cuts, the shape of the background, and the uncertainty from the total number of $\psi(2S)$ events. Compared with the corresponding branching fraction from J/ψ decay, this result is consistent with the "12%" rule [8], as shown in Table I.

A $f_0(1710)$ signal is observed in the $\pi^+\pi^-$ invariant mass distribution, as shown in Fig. 2(a). The number of $f_0(1710)$ events above background is 35.6 ± 4.8. The Monte Carlo determined efficiency for this channel is 45.4%, and the resulting branching fractions are

$$B(\psi(2S) \to \gamma f_0(1710)) \times B(f_0(1710) \to \pi\pi)$$

$$= (3.01 \pm 0.41 \pm 1.24) \times 10^{-5}.$$

The region with a $\pi^+\pi^-$ invariant mass greater than 3 GeV has been presented elsewhere [13]. The region with a $\pi^0\pi^0$ invariant mass greater than 3 GeV [see Fig. 3(a)] has signal peaks due to the χ_{c0} and χ_{c2} charmonium states. This mass distribution is fitted with two Breit-Wigner resonances plus a polynomial background function, and 96.9 ± 11.1 and 20.8 ± 5.8 events are obtained for χ_{c0} and χ_{c2}, respectively. The detection efficiencies are 10.5% and 8.2%, and the resulting branching fractions are

$$B(\chi_{c0} \to \pi^0\pi^0) = (2.79 \pm 0.32 \pm 0.57) \times 10^{-3}$$

and

$$B(\chi_{c2} \to \pi^0\pi^0) = (9.8 \pm 2.7 \pm 5.6) \times 10^{-4}.$$

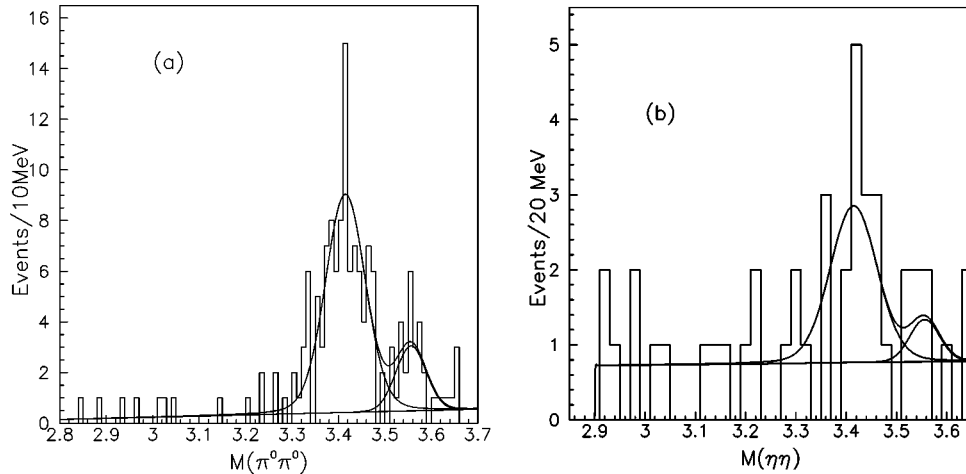The detection efficiencies, branching fraction acceptances, and final results for the decays described in this section are summarized in Tables II–V.

V. $\psi(2S) \to \gamma K\bar{K}$ ANALYSIS

Here the analysis of decays into charged and neutral kaon pairs, $\psi(2S) \to \gamma K^+ K^-$ and $\psi(2S) \to \gamma K_S^0 K_S^0 \to \gamma 4\pi^\pm$, is presented. For the $\psi(2S) \to \gamma K^+ K^-$ channel, cuts similar to those for the $\gamma\pi^+\pi^-$ analysis are used, but with the requirement that the combined probability of particle identification and kinematic fit for two kaon hypothesis should be greater than 1% and should be greater than the combined probability for the two pion hypothesis. QED backgrounds such as $e^+e^- \to \gamma\phi \to \gamma K^+ K^-$ and $e^+e^- \to \gamma\mu^+\mu^-$ are determined using the τ scan data (see Fig. 4). A $f_0(1710)$ signal and a hint of a possible $f_2'(1525)$ signal (Fig. 5) are observed. The mass distribution is fitted using S-wave and D-wave Breit-Wigner functions with masses and widths fixed at the PDG values for $f_0(1710)$ and $f_2'(1525)$, respectively. The fit yields 39.6 ± 5.9 $f_0(1710)$ events above background. The detection efficiency is 33.6%, giving a branching fraction

$$B(\psi(2S) \to \gamma f_0(1710)) \times B(f_0(1710)$$

$$\to K^+ K^-)$$

$$= (3.02 \pm 0.45 \pm 0.66) \times 10^{-5}.$$

The systematic error includes the uncertainties from varying the cuts and the total number of $\psi(2S)$'s. The uncertainties

FIG. 3. Invariant mass of (a) $\pi^0\pi^0$ and (b) $\eta\eta$. The curves are Breit-Wigner functions to describe the $\chi_c 0$ and $\chi_c 2$ along with a polynomial to describe the background.

TABLE II. Numbers of events before and after correction for efficiency and branching fraction acceptance. Branching fraction acceptance factors include branching fractions from intermediate decays processes such as $\pi^0 \to \gamma\gamma$, $\eta \to \gamma\gamma$, $K_S^0 \to \pi^+\pi^-$, $f_2(1270) \to \pi\pi$, etc. They do not include iso-spin factors.

Mode	Number of events from mass fitting	Detection efficiency	Branching fractions correction factor	Number of events after correction
$\psi(2S) \to \gamma f_2(1270)$ from $\gamma\pi^+\pi^-$	200.8 ± 18.8	43.8%	0.847 ± 0.024	$540.7 \pm 50.6 \pm 81.9$
$\psi(2S) \to \gamma f_2(1270)$ from $\gamma\pi^0\pi^0$	29.9 ± 11.1	9.6%	0.827 ± 0.028	$376.7 \pm 139.9 \pm 138.1$
$\psi(2S) \to \gamma f_0(1710) \to \gamma\pi\pi$ from $\gamma\pi^+\pi^-$	35.6 ± 4.8	45.4%	1.0 ± 0.0	$78.4 \pm 10.7 \pm 32.0$
$\psi(2S) \to \gamma f_0(1710) \to \gamma K^+ K^-$	39.6 ± 5.9	33.6%	1.0 ± 0.0	$117.9 \pm 17.6 \pm 24.9$
$\psi(2S) \to \gamma f_0(1710) \to \gamma K_S^0 K_S^0$	6.8 ± 3.1	18.0%	0.471 ± 0.003	$80.3 \pm 36.6 \pm 41.9$

TABLE III. Branching fractions and ratios of branching fractions $[B/B(\psi(2S) \to \pi^+\pi^- J/\psi)]$ for $\psi(2S) \to \gamma X \to \gamma P\bar{P}$ modes (P stands for pseudo-scalar).

Mode	$B(\times 10^{-4})$	$B/B(\psi(2S) \to \pi^+\pi^- J/\psi)(\times 10^{-4})$
$\psi(2S) \to \gamma f_2(1270)$ from $\gamma\pi^+\pi^-$	$2.08 \pm 0.19 \pm 0.33$	$6.82 \pm 0.64 \pm 1.04$
$\psi(2S) \to \gamma f_2(1270)$ from $\gamma\pi^0\pi^0$	$2.90 \pm 1.08 \pm 1.07$	$9.52 \pm 3.53 \pm 3.49$
$\psi(2S) \to \gamma f_2(1270)$ from $\gamma\pi\pi$	$2.12 \pm 0.19 \pm 0.32$	$6.99 \pm 0.64 \pm 1.00$
$\psi(2S) \to \gamma f_0(1710) \to \gamma\pi\pi$ from $\gamma\pi^+\pi^-$	$0.301 \pm 0.041 \pm 0.124$	$0.99 \pm 0.14 \pm 0.40$
$\psi(2S) \to \gamma f_0(1710) \to \gamma K^+ K^-$	$0.302 \pm 0.045 \pm 0.066$	$0.99 \pm 0.15 \pm 0.21$
$\psi(2S) \to \gamma f_0(1710) \to \gamma K_S^0 K_S^0$	$0.206 \pm 0.094 \pm 0.108$	$0.68 \pm 0.31 \pm 0.35$

TABLE IV. Numbers of events corrected for efficiency and branching fraction acceptance for χ_c decay.

Mode	Number of event from mass fitting	Detection efficiency	Branching fractions correction factor	Number of events after correction
$\chi_{c0} \to \pi^0\pi^0$	96.9 ± 11.1	10.5%	0.9761 ± 0.0005	$945.4 \pm 108.3 \pm 163.8$
$\chi_{c2} \to \pi^0\pi^0$	20.8 ± 5.8	8.2%	0.9761 ± 0.0005	$259.9 \pm 72.5 \pm 145.8$
$\chi_{c0} \to \eta\eta$	12.7 ± 5.3	11.9%	0.1554 ± 0.0014	$686.3 \pm 286.4 \pm 187.9$
$\chi_{c2} \to \eta\eta$	<5.9	10.5%	0.1554	<361.3

TABLE V. The χ_c decay branching fractions, and ratios of branching fractions for $\chi_{c0,2} \to \pi^0\pi^0$ or $\eta\eta [B \times B(\psi(2S) \to \gamma\chi_{c0,2})/B(\psi(2S) \to \pi^+\pi^- J/\psi)]$.

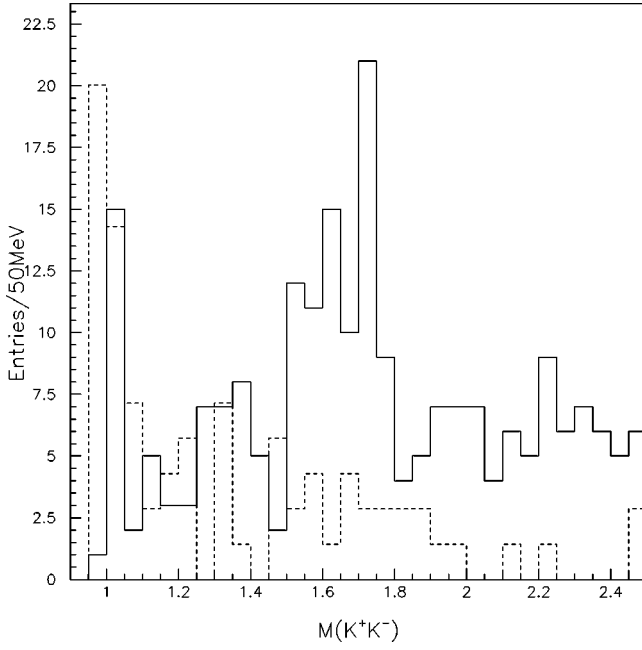| Mode	$B(\times 10^{-3})$	$B \times B(\psi(2S) \to \gamma\chi_{c0,2})(\times 10^{-4})$	$B \times B(\psi(2S) \to \gamma\chi_{c0,2})/B(\psi(2S) \to \pi^+\pi^- J/\psi)(\times 10^{-4})$
$\chi_{c0} \to \pi^0\pi^0$	$2.79 \pm 0.32 \pm 0.57$	$2.42 \pm 0.28 \pm 0.44$	$7.96 \pm 0.91 \pm 1.38$
$\chi_{c2} \to \pi^0\pi^0$	$0.98 \pm 0.27 \pm 0.56$	$0.67 \pm 0.19 \pm 0.38$	$2.19 \pm 0.61 \pm 1.23$
$\chi_{c0} \to \eta\eta$	$2.02 \pm 0.84 \pm 0.59$	$1.76 \pm 0.73 \pm 0.49$	$5.78 \pm 2.41 \pm 1.58$
$\chi_{c2} \to \eta\eta$	<1.37	<0.93	<3.04

FIG. 4. $M_{K^+K^-}$ distributions. The solid line histogram is the distribution for the $\psi(2S)$ data; the dashed histogram is that for the normalized τ data.

of the mass and width of $f_0(1710)$ also contribute to the systematic error. This result is again consistent with the "12%" rule. See Table I.

For the $\psi(2S) \to \gamma K_S^0 K_S^0 \to \gamma \pi^+ \pi^- \pi^+ \pi^-$ channel, events with two positive charged tracks, two negative charged tracks and at least one photon are selected. Both K_S^0 vertices are reconstructed and $|M_{\pi^+\pi^-} - M_{K_S^0}|$ must be smaller than 20 MeV. At least one of the combinations must yield a four-constraint fit with χ^2 probability greater than 0.01. If more than one combination survives, the combination with the smallest value of

$$\sqrt{(m_{\pi_1^+\pi_2^-} - m_{K_S^0})^2 + (m_{\pi_3^+\pi_4^-} - m_{K_S^0})^2}$$

is chosen. An S-wave Breit Wigner plus a polynomial background are used to fit the invariant mass distribution shown in Fig. 5(b). The fit finds 6.8 ± 3.1 events, or an upper limit of 10.8 events at the 90% confidence level. The detection efficiency for this channel is 18.0%. The branching fraction is

$$B(\psi(2S) \to \gamma f_0(1710)) \times B(f_0(1710)$$
$$\to K_S^0 K_S^0)$$
$$= (2.06 \pm 0.94 \pm 1.08) \times 10^{-5}$$

or

$$< 3.89 \times 10^{-5} \quad (90\% \text{ C.L.}).$$

The detection efficiencies, branching fraction acceptances, and final results for the decays described in this section are summarized in Tables II to V.

VI. $\psi(2s) \to \gamma \eta \eta$ ANALYSIS

Here the analysis of decays into η pairs, $\psi(2S) \to \gamma \eta \eta \to 5\gamma$, is presented. The selection criteria for this channel are similar to those used in the $\psi(2S) \to \gamma \pi^0 \pi^0$ channel except that the requirement $|M_{\gamma\gamma} - M_\eta| < 70$ MeV is imposed. In the region where $M_{\eta\eta} < 3$ GeV, no $\eta\eta$ resonant state is observed. In the mass region with $M_{\eta\eta} > 3$ GeV, shown in Fig. 3(b), a χ_{c0} signal and a possible χ_{c2} signal are observed. Two Breit-Wigner functions with a polynomial background are used to fit the mass distribution, and 12.7 ± 5.3 events for χ_{c0} and an upper limit of 5.9 χ_{c2} events are found, giving the following branching fractions

$$B(\chi_{c0} \to \eta\eta) = (2.02 \pm 0.84 \pm 0.59) \times 10^{-3}$$

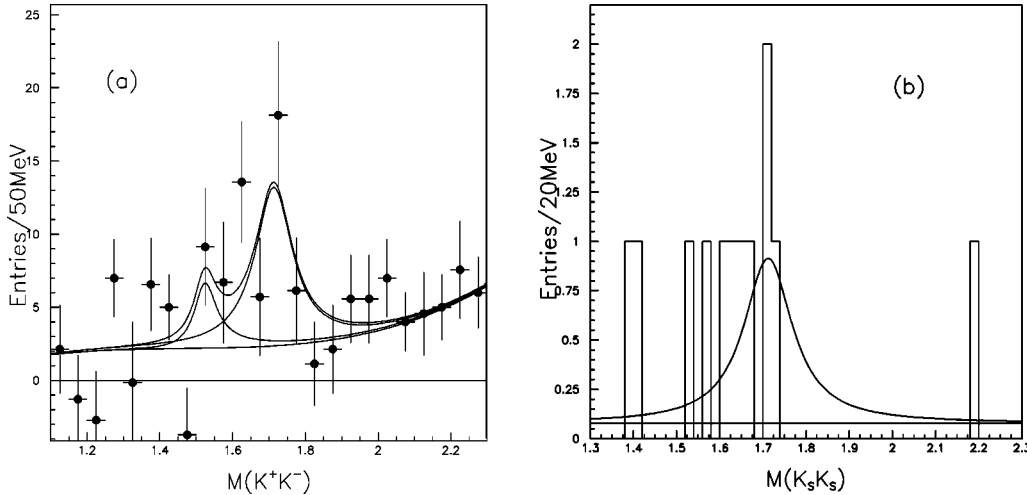$$B(\chi_{c2} \to \eta\eta) < 1.37 \times 10^{-3} \quad (90\% \text{ C.L.}).$$

FIG. 5. (a) $M_{K^+K^-}$ fit result. The data points are obtained from the difference of the two histograms in Fig. 4. The curves are Breit-Wigner functions to describe the $f_2'(1525)$ and the $f_0(1710)$ with a polynomial to describe the background. (b) $M_{K_S^0 K_S^0}$ fit result. The curves are a Breit-Wigner function for the $f_0(1710)$ and a polynomial for the background.

The detection efficiencies for these two channels are 11.9% and 10.5%, respectively.

Flavor SU(3) symmetry predicts that the branching fractions of χ_{c0} decay into $\pi^0\pi^0$ and $\eta\eta$ should be the same except for a phase space factor and a barrier factor of $p^{(2s+1)}$, where p is the momentum of the π^0 or η in χ_c's rest frame and s is the spin of the χ_c. Based on the PDG values for the χ_{c0}, this predicts $B(\chi_{c0}\rightarrow\eta\eta)/B(\chi_{c0}\rightarrow\pi^0\pi^0)$ $=0.95$ which is consistent with our measurement of

$$\frac{B(\chi_{c0}\rightarrow\eta\eta)}{B(\chi_{c0}\rightarrow\pi^0\pi^0)}=0.73\pm0.30\pm0.25.$$

The detection efficiencies, branching fraction acceptances, and final results for the decays described in this section are summarized in Tables II to V.

VII. SUMMARY

This paper studies $\psi(2S)\rightarrow\gamma\pi^+\pi^-$, $\gamma\pi^0\pi^0$, γK^+K^-, $\gamma K_S^0 K_S^0$, $\gamma\eta\eta$ final states and reports the first measurement of the $\psi(2S)\rightarrow\gamma f_2(1270)$ and $\psi(2S)\rightarrow\gamma f_0(1710)$ $\rightarrow\gamma K^+K^-$ and $\gamma K_S^0 K_S^0$ branching fractions. A clear $f_0(1710)$ signal in $\psi(2S)$ radiative decay into K^+K^- final states is observed. The results are consistent with the "12%" rule.

In addition, this paper reports the first measurement of the branching fractions of χ_{c0} and χ_{c2} decay into $\pi^0\pi^0$, χ_{c0} decay into $\eta\eta$, and an upper limit of the branching fraction of χ_{c2} decay into $\eta\eta$. The results from $\chi_{c0}\rightarrow\pi^0\pi^0$ and $\eta\eta$ are consistent with the prediction by SU(3) flavor symmetry.

[1] W.S. Hou and A. Soni, Phys. Rev. Lett. **50**, 569 (1980); G. Karl and W. Roberts, Phys. Lett. **144B**, 243 (1984); S.J. Brodsky *et al.*, Phys. Rev. Lett. **59**, 621 (1987); M. Chaichian *et al.*, Nucl. Phys. **B323**, 75 (1989); S. S Pinsky, Phys. Lett. B **236**, 479 (1990); X.Q. Li *et al.*, Phys. Rev. D **55**, 1421 (1997); S.J. Brodsky and M. Karliner, Phys. Rev. Lett. **78**, 4682 (1997); Y.Q. Chen and E. Braaten, *ibid.* **80**, 5060 (1998).

[2] M.E.B. Franklin *et al.*, Phys. Rev. Lett. **51**, 11 (1983).

[3] BES Collaboration, J.Z. Bai *et al.*, Phys. Rev. Lett. **81**, 5080 (1999).

[4] T. Appelquist, A. De Rújula, H.D. Politzer, and S.L. Glashow, Phys. Rev. Lett. **34**, 365 (1975); M. Chanowitz, Phys. Rev. D **12**, 918 (1975); L. Okun and M. Voloshin, ITEP-95-1976 (unpublished); S.J. Brodsky, T.A. DeGrand, R.R. Horgun, and D.G. Coyne, Phys. Lett. **73B**, 203 (1978); K. Koller and T. Walsh, Nucl. Phys. **B140**, 449 (1978).

[5] D. Aston *et al.*, Nucl. Phys. **B301**, 525 (1988); D. Aston *et al.*, Phys. Lett. B **215**, 199 (1988).

[6] The total number of $\psi(2S)$ recorded by the BES detector is determined by the total number of $\psi(2S)\rightarrow\pi^+\pi^- J/\psi$ events divided by the PDG branching fraction value for this mode. This total $\psi(2S)$ number is $(4.02\pm0.22)\times10^6$. In this paper, only runs of good quality have been used, corresponding to $3.90\pm0.21\times10^6\psi(2S)$ events and $1.188\pm0.003\pm0.016$ $\times10^6$ $\pi^+\pi^- J/\psi$ events. [8,9]. Please note that those numbers in reference paper [9] are obtained using a 1996 Particle Data Group publication [10].

[7] BES Collaboration, J.Z. Bai *et al.*, Nucl. Instrum. Methods Phys. Res. A **344**, 319 (1994).

[8] Particle Data Group, K. Hagiwara *et al.*, Phys. Rev. D **66**, 010001 (2002).

[9] BES Collaboration, J.Z. Bai *et al.*, Phys. Rev. D **58**, 092006 (1998).

[10] Particle Data Group, R.M. Barnett *et al.*, Phys. Rev. D **54**, 1 (1996).

[11] BES Collaboration, J.Z. Bai *et al.*, Phys. Rev. D **53**, 20 (1996).

[12] The 90% C.L. limits are calculated by increasing the number of events from the fit by 1.28σ, where σ includes the statistical error and the systematic error added in quadrature.

[13] BES Collaboration, J.Z. Bai *et al.*, Phys. Rev. Lett. **81**, 3091 (1998).